Redox Biology 56 (2022) 102461

Contents lists available at ScienceDirect

Redox Biology

journal homepage: www.elsevier.com/locate/redox

HDAC11 negatively regulates antifungal immunity by inhibiting *Nos2* expression via binding with transcriptional repressor STAT3

Han Wu [1], Xiaofan Yin [1], Xibao Zhao, Zherui Wu, Yue Xiao, Qianqian Di, Ping Sun, Haimei Tang, Jiazheng Quan, Weilin Chen [*]

Guangdong Provincial Key Laboratory of Regional Immunity and Diseases, Institute of Biological Therapy, Department of Immunology, Shenzhen University School of Medicine, Shenzhen, China

ARTICLE INFO

Keywords:
Histone deacetylase 11
Fungal infection
Candida albicans
Nos2
STAT3

ABSTRACT

Fungal infections cause serious health problems, especially in patients with an immune-deficiency. Histone deacetylase 11 (HDAC11) mediates various immune functions, yet little is known about its role in regulating host immune responses to fungal infection. Here we report that HDAC11 negatively controls antifungal immunity in macrophages and dendritic cells. Deleting *Hdac11* protects mice from morbidity and markedly improves their survival rate upon systemic infection with *Candida albicans* (*C. albicans*). Moreover, HDAC11 deficiency results in increased production of NO and reactive oxygen species, which enhances fungal killing. Mechanistically, loss of HDAC11 increases histone 3 and 4 acetylation at the *Nos2* promoter and leads to enhanced *Nos2* transcription and corresponding iNOS levels in macrophages. In addition, STAT3, a transcriptional repressor of *Nos2*, physically interacts with HDAC11, serving as a scaffold protein supporting the HDAC11 association with the *Nos2* promoter. Notably, treatment with the HDAC11 inhibitor, FT895, exhibits antifungal therapeutic effects in both mouse and human cells challenged with *C. albicans*. These data support that HDAC11 may be a therapeutic target for fungal infection.

1. Introduction

Fungal infections cause serious health problems, especially in people with an immunodeficiency status, including patients with AIDS, autoimmune diseases, or patients undergoing anticancer chemotherapy or organ transplantation [1,2]. Many fungi genera have been isolated from patients: *Candida albicans* (*C. albicans*) is the most important fungal pathogen, causing both mucosal and systemic fungal infections [3]. Despite the availability of several antifungal drugs, the high rate of mortality associated with invasive fungal infections remains a major concern [1]. The development of new antifungal drugs over recent years has been insufficient; meanwhile, antifungal drug resistance is growing and further threatens the limited agents of antifungals available to treat these serious infections [2,4]. Therefore, improving our understanding of the immune response toward *C. albicans* is crucial to develop novel therapeutic strategies to combat candidiasis.

Phagocytes, including macrophages and dendritic cells (DCs), provide the first line of defense against invasive pathogens and are important for the activation and regulation of the innate immune response. These cells express several classes of pattern recognition receptors (PRR), including the Toll-like receptors (TLRs), C-type lectin receptors (CLRs), NOD-like receptors (NLRs), and RIG-I-like receptors (RLRs). These receptors recognize distinct components of invading pathogens, termed pathogen-associated molecular patterns (PAMPs) [5]. The best-characterized PRRs in fungi sensing are the CLRs members [6–8], such as dectin-1, dectin-2, and macrophage-inducible C-type lectin (mincle). The three main cell wall components presented in almost all pathogenic fungi are β-glucans, α-mannan, and chitin, which can be recognized by dectin-1, dectin-2/3, and mincle, respectively. Some TLRs, such as TLR2 and TLR4, also recognize the fungi cell wall components phospholipomannans and glucuronoxylomannan [9]. Once activated, PRRs on phagocytes initiate downstream intracellular events that lead to the production of cytokines and other mediators, which ultimately facilitate the elimination of infectious fungi [10]. Dectin-1 directly interacts with and activates the spleen tyrosine kinase (SYK), triggering the caspase recruitment domain containing protein 9

* Corresponding author.
E-mail address: cwl@szu.edu.cn (W. Chen).
[1] These authors contribute equally to this work.

https://doi.org/10.1016/j.redox.2022.102461
Received 10 August 2022; Accepted 25 August 2022
Available online 3 September 2022

(CARD9) pathway. Unlike dectin-1, both dectin-2 and mincle activate SYK indirectly by complexing with the adaptor protein Fc receptor γ-chain (FcRγ) [11,12]. SYK-CARD9 signaling further triggers NF-κB and MAPK pathway activation. The three major MAPK pathways activated by PRRs are c-Jun N-terminal kinase (JNK), p38 and extracellular signal-regulated kinase (ERK). Recently, *in vivo* studies in mouse models with systemic fungal infection showed that p38γ/p38δ or JNK1 deficiency protects against *C. albicans* infection [13,14].

Histone deacetylases (HDACs) remove acetyl groups from histone and non-histone lysine residues [15]. HDACs are categorized into four major classes based on structure and function [16], namely class I HDACs (HDAC1, 2, 3, 8), class II HDACs (HDAC4, 5, 6, 7, 9, 10), class III HDACs (SIRT1-7) and class IV HDAC (HDAC11). Being the only class IV HDAC, HDAC11 has crucial roles in various cellular events, such as cell proliferation and differentiation, metabolism, and tumorigenesis [17–20]. HDAC11 is highly expressed in multiple immune cells, including phagocytes, neutrophils, T cells, and B cells [21–24]. HDAC11 was initially characterized as a negative regulator of the interleukin 10 (IL-10) in macrophages [23], but an HDAC11 deficiency in mice promotes neutrophil and T-cell response [21,24]. Besides its shared HDAC family catalytical activity, HDAC11 is a multifaceted enzyme with efficient defatty acylase activity [25].

Although recent observations have uncovered multiple roles of HDAC11 in innate and adaptive systems [16], the role of HDAC11 in host antifungal immunity has not been studied. Here we reported that HDAC11 negatively regulates the host antifungal immune response through repressing *Nos2* expression and NO production, which may serve as a potential target for treating fungal diseases.

2. Materials and methods

2.1. Antibodies and reagents

Heat-killed *C. albicans* (HKCA; tlrl-hkca), zymosan (tlrl-zyn) and Trehalose-6,6-dibehenate (TDB; tlrl-tdb) were purchased from Invivogen. Mannan (M3640) were purchased from Sigma-Aldrich. The HDAC11 inhibitors FT895 (HY-112285) and SIS17 (HY-128918), SYK inhibitor R406 (HY-12067), NF-κB inhibitor JSH-23 (HY-13982) and STAT3 inhibitor STAT3-IN-1 (HY-100753) were purchased from MedChemExpress. iNOS inhibitors S-methylisothiourea hemisulfate salt (SMT; S0008) and L-NMMA (S0011) were purchased from Beyotime Biotechnology. The SYK inhibitor R406 (S2194) was purchased from Selleck. The antibodies used in this study shown in Supplementary Table 1.

2.2. Mice

Hdac11 conventional knockout (*Hdac11*$^{-/-}$) mice with a C57BL/6 background were purchased from Cyagen Bioscience (Suzhou, China). Wild-type (*Hdac11*$^{+/+}$) littermates and *Hdac11*$^{-/-}$ mice were obtained by crossing *Hdac11* heterozygous mice. The mice were maintained in a specific pathogen-free facility with a 12 h/12 h light/dark cycle.

2.3. Cells

The HEK-293T cell and human monocytic cell line THP-1 were purchased from the Cell Resource Center of Institute of Basic Medicine, Chinese Academy of Medical Sciences. HEK-293T cells were cultured in DMEM containing 10% fetal bovine serum (FBS) and 1% penicillin and streptomycin (PS). THP-1 cells were cultured in RIPM-1640 containing 10% FBS and 1% PS. Before treatment, THP-1 cells were induced to form macrophages with 20 ng/mL PMA for 2 days.

Mouse primary bone marrow (BM)-derived macrophages (BMDM) and BM-derived dendritic cells (BMDC) were prepared and cultured following the previous protocols [26].

To prepare human monocyte-derived macrophages, human peripheral blood mononuclear cells (PBMC) were isolated from fresh peripheral blood from healthy donors with Ficoll (Merck) based on a density gradient centrifugation. PBMC were cultured in RIPM-1640 containing 10% FBS, 1% PS and 20 ng/mL recombinant human granulocyte-macrophage colony-stimulating factor (rhGM-CSF; Peprotech) for 6 days. The medium was half-changed every 2 days.

2.4. Plasmids

The full-length coding sequence for mouse *Hdac11* was cloned using cDNA from mouse macrophages as a template. The PCR-amplified fragment was inserted into pcDNA3.1 vector carrying a Flag- or Myc-tag between the BamHI and XhoI sites. *Hdac11* mutant plasmid with two site mutations (D181A/H183A) was sub-cloned using a Hieff Mut™ Site-Directed Mutagenesis Kit (11003ES10; YEASEN). Adenoviruses carrying WT and mutant *Hdac11* constructs for overexpression were obtained from OBIO Technology. Using mouse genomic DNA as a template, the *Nos2* promoter was amplified in various lengths, including 1755 bp (−1555 to +200), 1054 bp (−854 to +200), and 500 bp (−300 to +200). The PCR products were cloned into the pGL3-enhancer vector digested with XhoI to generate the plasmids *Nos2*-pro1755-luc, *Nos2*-pro1054-luc and *Nos2*-pro500-luc, respectively. Other expression vectors were constructed according to the standard method as above. The cloning primers are shown in Supplementary Table 2.

2.5. Bone marrow-chimeric mice

Eight-week-old recipient mice were irradiated by 8 Gy X-ray, and after 6 h 5 × 10^6 BM leukocytes from donors were intravenously transferred to the mice. Chimeric mice were used for further experiments 8 weeks after the initial BM transplantation.

2.6. Adoptive transplantation of BMDM

Eight-week-old weight match mice were injected intraperitoneally with 200 μl clodronate liposomes (40337ES08, YEASEN) to delete macrophage *in vivo*, and injected with equal volume of PBS liposomes (40338ES05, YEASEN) as control, and handled according to the manufacturer's instructions. Fourty-8 h later, 2 × 10^6 BMDM cells were intravenously transferred for each mice. After a further 12 h mice were used for further experiments.

2.7. In vivo neutrophil depletion based on antibody treatment

Rat anti-Ly6G (clone RB6-8C5, #BE0075) and rat IgG2a isotype control (#BP0089) were purchased from Bio X Cell. For *in vivo* neutrophil depletion, 100 μg anti-Ly6G antibody was intraperitoneally injected per mouse, and IgG isotype control was use as control. After 24 h, the treated mice were used for further experiments and analysis.

2.8. Systemic candidiasis model

For systemic *C. albicans* infection, mice were injected via the tail vein with a suspension containing different doses of *C. albicans* (SC5314 strain) in 200 μl of sterile PBS. Mouse survival and weight were monitored following infection. The fungal load was assessed by plating a series of diluted solutions of homogenized kidneys on yeast extract peptone dextrose (YPD) plates.

2.9. Quantitative PCR

Total RNA was extracted with Trizol reagent (Takara) by following the manufacturer's instructions. Reverse transcription was performed using reverse transcriptase M-MLV (RNase H-; Takara). Real-time quantitative PCR was performed with Hieff™ qPCR SYBR Green Master Mix (Yeasen) on Analytik Jena qTOWER3 PCR system (Jena,

Germany). The relative mRNA levels were determined by normalization of expression of β-actin in each sample. The gene-specific primer sequences are listed in Supplementary Table 2.

2.10. Immunoprecipitation and immunoblot analysis

For immunoprecipitation in HEK293T cells, cell lysates were incubated with Flag M2 or Myc magnetic beads for 2 h at 4 °C. For immunoprecipitation of endogenous proteins, BMDM cells were stimulated with 100 μg/mL zymosan for 1 h before lysis with 0.5% NP40 buffer containing 1% protease inhibitor cocktail (MedChemExpress). BMDM cell lysates were immunoprecipitated overnight with specific antibodies and then pulled down using Protein A/G magnetic beads (Bimake). Precipitates were analyzed by immunoblotting using the indicated antibodies.

For immunoblot analysis, total proteins from tissues or cells were prepared using RIPA buffer (Beyotime Biotechnology) containing 1% protease inhibitor cocktail. The protein concentrations were determined using a BCA assay kit (Pierce Biotechnology). Proteins were separated on SDS-PAGE gels and were electrotransferred onto nitrocellulose filter membranes (Millipore). The membranes were blocked with 5% non-fat milk at room temperature for 1 h and then incubated with the indicated primary antibodies overnight at 4 °C, followed by their respective secondary antibodies. Detection was performed using an Enhanced ECL Western Blot Substrates Reagent kit (ThermoFisher Scientific). Band densitometry was quantified by ImageJ software.

2.11. Cytokines measurement

Murine kidney tissue was lysed in 100 mg tissue/mL PBS with 1% proteinase inhibitor cocktails and grinded with the procedure of 20 s/20 s for 5 cycles by Tissue Lyser (DHSBio, China). The supernatants were collected after centrifugation at 8000*g* for 10 min. The supernatants were used to monitor TNF-α, IL-6 or IL-1β concentrations by ELISA according to the manufacturer's instructions (Invitrogen).

2.12. Chromatin immunoprecipitation (ChIP) assays

ChIP assay was performed according to the manufacturer's procedures (Merck Millipore, Cat. 17-371) and as previously described [23]. The enrichments of DNA were analyzed by quantitative PCR. The PCR primers used are listed in Supplementary Table 2.

2.13. Luciferase reporter assays

HEK293T cells were transfected with 100 ng of the luciferase (firefly) reporter plasmid pGL3 containing indicated length of the *Nos2* promoter, together with 10 ng of the reference *Renilla* luciferase reporter, and with or without 50 ng of an activated *Syk* expression plasmid. The transfected cells were further cultured in DMEM containing 10% FBS for 24 h. The cells were collected and lysed, and firefly and *Renilla* luciferase activities were measured with the Dual-Luciferase Reporter System (Promega). The *Renilla* luciferase activity was used to normalize for transfection efficiency.

2.14. Histopathology

For histopathology analysis, murine kidneys were fixed in a 10% formaldehyde solution, and embedded in paraffin and sectioned according to standard procedures. 5-μm sections were stained with hematoxylin and eosin (H&E), periodic acid-schiff (PAS), or were used for immunohistochemical staining with specific antibodies. Stained sections were scanned using a K-Viewer Digital Imaging System (KFBIO Tech), and evaluated for severity of inflammation and intralesional fungal burden as previously described [13]. Renal inflammation was scored based on H&E and PAS staining (proportion of renal parenchyma and/or pelvis involved by tubulointerstitial nephritis/pyelonephritis) as not significant (score 0), less than 10% (score 1), 10–25% (score 2), 25–50% (score 3) or greater than 50% (score 4). The intralesional fungal burden score was based on PAS staining and defined as not significant (score 0), scant presence in less than 10% of inflammatory foci (score 1), mild-to-moderate presence in 10–25% of inflammatory foci (score 2), moderate-to-significant presence in 25–50% of inflammatory foci (score 3) or significant presence in more than 50% of inflammatory foci (score 4). ImageJ software was applied to evaluate the extent of Ly-6G$^+$ cell infiltration into the affected kidneys. Regions and cells of interest were manually classified in representative areas of slides to identify Ly-6G positive target objects based on the morphology and positive immunohistochemical staining. At least eight randomly selected fields of each slide were used for Ly-6G$^+$ cells analyses.

2.15. Detection of nitric oxide (NO) production

Cell culture supernatants were collected and the concentration of NO was measured using an NO assay kit (S0021, Beyotime Biotechnology) based on the Griess reaction. All samples were prepared according to the manufacturer's protocol.

2.16. Measurement of reactive oxygen species (ROS) production

Production of ROS was measured using luminol as the probe in real time over 120 min as previously described but with minor modification [14]. Briefly, 1×10^5 cells were plated in 96-well sterile luminometer plate (Costar) with 200 μL culture medium (0.05% FBS in HBSS). Cells were stimulated or not as indicated, with a final concentration of 7.5 μg/well L-012 (Wako Chemicals) incorporated in the medium at the beginning of the stimulation. Chemiluminescence was measured at 2-min intervals and expressed as relative light units (RLU).

2.17. Phagocytosis of C. albicans and fungal killing assays

A phagocytosis assay was performed as previously described [13]. Briefly, 5×10^5 BMDM cells were cultured in 12-well plate, and 5×10^5 CFU live *C. albicans* (1 MOI) were added and incubated for 30 min at 37 °C. Then the supernatant was collected and the cells were washed gently with RIPM-1640 three times to remove unphagocytized *C. albicans*. The supernatant and well wash medium were combined and plated in serial dilutions on YPD plates. The percentage of phagocytized microorganisms was defined as (1 – (CFU of unphagocytized *C. albicans*/CFU at the start of incubation)) × 100.

A fungal killing assay was performed as previously described but with minor modifications [27]. Briefly, cells were incubated with 0.5 MOI live *C. albicans* for 30 min at 30 °C. After unbound microorganisms were removed by gently washing with RIPM-1640 medium, the cells were returned to the incubator for 4 h to allow fungal killing. The control plates were kept at 4 °C to measure live microorganisms in the wells. After incubation, the medium was removed and the cells were lysed by incubation with sterile water (pH = 11.0) for 5 min. Lysis buffer was neutralized with excess PBS, and the titer was determined by plating on YPD agar plates.

2.18. Ethics statement

Human peripheral blood was donated by healthy individuals who obtained written informed consent. Animal experiments were carried out according to the National Institute of Health Guide for the Care and Use of Laboratory Animals. And all the experimental protocols were reviewed and approved by Ethics Committee of Shenzhen University (Approval No. 2021011).

2.19. Statistical analysis

The data are presented as the means ± SEM of at least triplicate experiments or means ± SD unless, as stated. Statistical difference between two groups was conducted using Student's *t*-test. A one-way ANOVA with Bonferroni's (selected pairs) post hoc test was used to compare more than two groups. A Dunnett's multiple comparisons test was used in mixed-effects analysis. The calculations were performed with Graphpad Prism 8 software. Statistical significance was set based on the *p* value, $*p < 0.05$, $**p < 0.01$, $***p < 0.001$.

3. Results

3.1. HDAC11 negatively regulates the host antifungal immune response

To investigate the roles of HDAC11 in the host immune response to fungal infection, we intravenously infected *Hdac11*$^{+/+}$ and *Hdac11*$^{-/-}$ mice with a sub-lethal dose of *C. albicans*. We found that *Hdac11*$^{-/-}$ mice were more resistant to fungal infection compared to *Hdac11*$^{+/+}$ control mice (Fig. 1A and B). Moreover, the fungal titers in kidneys of *Hdac11*$^{-/-}$ mice after systemic infection were significantly lower than that in *Hdac11*$^{+/+}$ mice (Fig. 1C). *Hdac11*$^{-/-}$ mice also exhibited attenuated renal inflammation and reduced numbers of fungi and neutrophils infiltration in the kidney (Fig. 1D and E). These data suggest that loss of HDAC11 in the host leads to an enhanced host antifungal immune response.

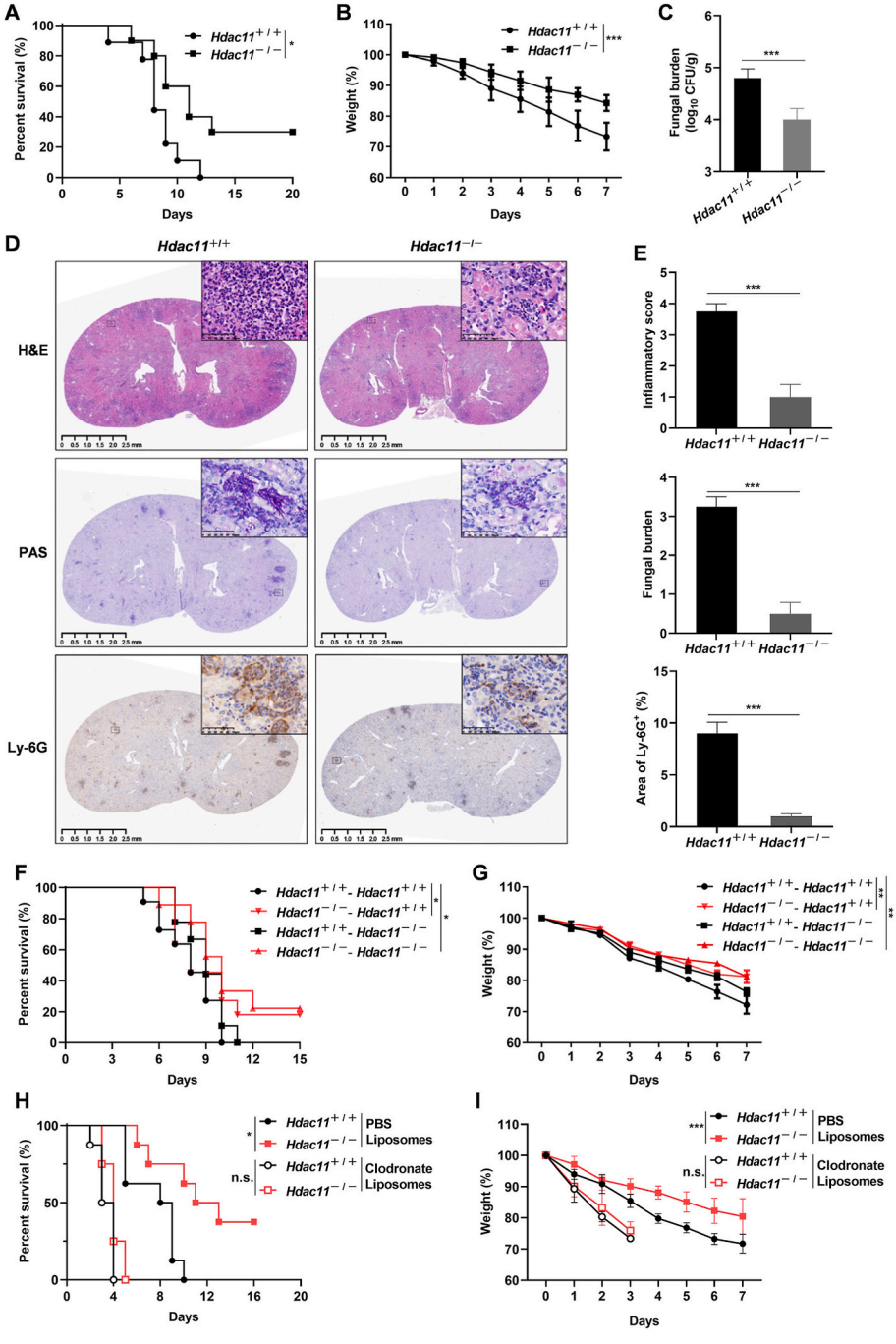

Fig. 1. *Hdac11* negatively regulates antifungal immunity. (A, B) *Hdac11*$^{+/+}$ (n = 9) and *Hdac11*$^{-/-}$ (n = 10) mice were intravenously infected with 2×10^5 CFU of *C. albicans* per mouse and monitored over time. (A) Survival and (B) weight loss were monitored after infection. (C) Fungal burdens in kidney 2 days after *C.albicans* infection. *Hdac11*$^{+/+}$ (n = 4) and *Hdac11*$^{-/-}$ (n = 3) mice were used, respectively. (D) Kidney sections from *Hdac11*$^{+/+}$ and *Hdac11*$^{-/-}$ mice infected with *C.albicans* as in (C) were stained with hematoxylin and eosin (H&E), periodic acid-schiff (PAS) or the neutrophil marker Ly-6G. Insets show regions of inflammation, fungal growth, and neutrophils infiltration, respectively. Representative images of at least three replicates are shown. Scale bar, 500 μm. (E) The inflammatory score based on renal immune cell infiltration/inflammation and tissue destruction, the fungal burden, and the percentage of the area positive for Ly-6G are shown. At least three mice for each group and three sections per kidney were analyzed. (F, G) Bone marrow-chimeric mice were prepared as described in the methods. The left and right genotypes shown in the panels indicate donor and irradiated mice, respectively. Age-matched male mice of *Hdac11*$^{+/+}$-*Hdac11*$^{+/+}$ (n = 11), *Hdac11*$^{+/+}$-*Hdac11*$^{-/-}$ (n = 9), *Hdac11*$^{-/-}$-*Hdac11*$^{+/+}$ (n = 11) and *Hdac11*$^{-/-}$-*Hdac11*$^{-/-}$ (n = 9) were used. Eight weeks after irradiation, mice were intravenously injected with 2×10^5 CFU of *C. albicans* per mouse. (F) Survival rate and (G) weight loss of these mice were monitored over time. (H, I) *Hdac11*$^{+/+}$ or *Hdac11*$^{-/-}$ mice were injected intraperitoneally with control PBS liposomes or clodronate liposomes 24 h before infected with 2×10^5 CFU of *C. albicans* for each mouse (n = 8 for each treatment). (H) Survival rate and (I) weight loss of these liposomes treated mice were monitored after infection. Data are shown as means ± SD. The *p* value for survival rate was assessed by log rank test and for loss of weight over time was assessed by Two-way ANOVA. And *p* value for two group comparison was calculated by Student's t-test. n.s., no significance, $*p < 0.05$, $**p < 0.01$, $***p < 0.001$.

HDAC11 is highly expressed in immune cells, including innate immune cells (such as macrophages and DCs) [23] and adaptive immune cells (T cells and B cells) [22,24]. However, we saw that loss of *Hdac11* barely affects the development of these immune cells *in vivo* (Supplementary Fig. 1). To gain insight into the cellular basis of HDAC11-associated antifungal immunity, we generated bone marrow (BM)-chimeric mice by reconstituting irradiated mice with syngeneic BM from *Hdac11*$^{+/+}$ or *Hdac11*$^{-/-}$ mice. Loss of *Hdac11* in hematopoietic cells showed a similar phenotype to that of conventional *Hdac11* deficiency in response to fungal infection (Fig. 1F and G). Due to the protective effect of *Hdac11* deficiency during the first few days after initial infection, we further determined the contribution of HDAC11 to the innate immune system. We generated mice deficient in phagocytes by clodronate liposomes inoculation [28]. Flow cytometry and immunohistochemical staining confirmed >90% clearance efficiency of macrophages in the spleen and kidney, respectively, after clodronate liposomes injection (Supplementary Fig. 2A and B). Compared with the control PBS liposome pre-treated *Hdac11*$^{+/+}$ mice, the *Hdac11*$^{-/-}$ cohorts showed a significant decrease in survival rate after challenged with *C. albicans*; however, the difference was abolished between clodronate liposomes pre-treated *Hdac11*$^{+/+}$ and *Hdac11*$^{-/-}$ groups, as evidenced by the mean survival period of both groups <4 days with no statistical difference ($p > 0.05$) (Fig. 1H). Likewise, the improvement in weight loss in *Hdac11*$^{-/-}$ mice compared to *Hdac11*$^{+/+}$ mice was abrogated after phagocyte depletion (Fig. 1I). Furthermore, adoptive transplantation of macrophages rescued the defense effect to fungal infection, as clodronate liposomes-treated mice transplanted with *Hdac11*$^{-/-}$ macrophages exhibited a lower fungal burden in the kidney when compared to mice transplanted with *Hdac11*$^{+/+}$ macrophages (Supplementary Fig. 2C). Neutrophils is another important mediator in the innate immune system for the prevention of fungal infection [29]. We generated mice with neutrophils deletion based on Ly6G antibody follow previous described [30]. Flow cytometry confirmed that Ly6G^{+} neutrophils in blood were almost completely removed, while Ly6C^{+} cells were barely affected (Supplementary Fig. 3A). PAS staining and fungal titer assay showed similar trends in *C. albicans* reduction in kidneys before and after neutrophils deletion (Supplementary Fig. 3B and C), suggesting that *Hdac11* deficiency mediated antifungal immunity in a neutrophil-independent manner *in vivo*. Together, our data indicated that *Hdac11* deficiency in phagocytic cells is critical for the observed beneficial effect in antifungal infection.

3.2. *Hdac11 deficiency elevates Nos2 expression and nitric oxide (NO) production*

Pro-inflammatory cytokines, such as IL-1β, IL-6, and IL-17, are key to the host defense against fungi infection [31,32]. Thus, we detected the mRNA levels of pro-inflammatory cytokines in kidney tissues from mice after *C. albicans* infection. We found that there were no differences in most cytokine levels, except for the upregulation of *Nos2* and *Cxcl1*, in *Hdac11*$^{-/-}$ mice when compared with *Hdac11*$^{+/+}$ mice (Supplementary Fig. 4A). Determination of the secretion of pro-inflammatory cytokines in the sera after fungal infection showed that IL-1β and IL-6, both of which enhance the host defense against fungi, were significantly decreased in *Hdac11*$^{-/-}$ mice compared to *Hdac11*$^{+/+}$ mice (Supplementary Fig. 4B). These data do not support the enhanced antifungal phenotype in *Hdac11*$^{-/-}$ mice. However, the levels of inducible nitric oxide synthase (iNOS), which is encoded by *Nos2*, were significantly higher in the kidneys of *Hdac11*$^{-/-}$ mice after fungal infection when compared with *Hdac11*$^{+/+}$ mice (Supplementary Fig. 4C). To validate

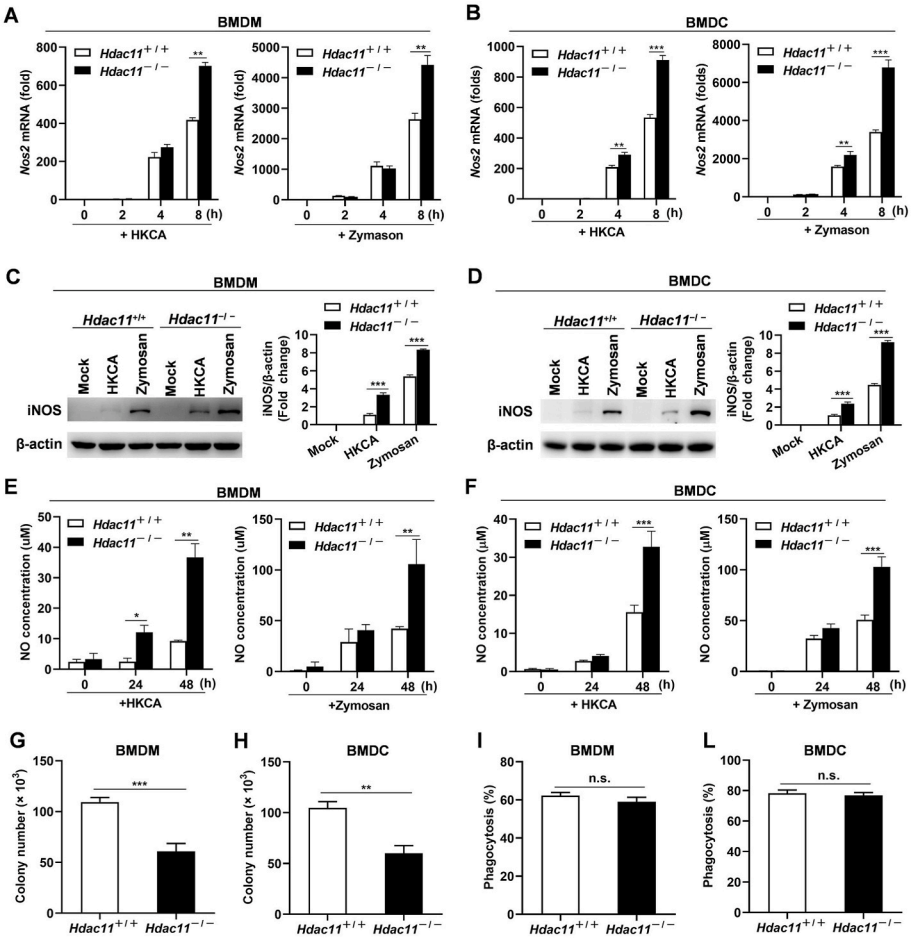

Fig. 2. *Hdac11*-deficiency elevates *Nos2* expression and NO production. (A, B) *Nos2* mRNA levels. (A) BMDM and (B) BMDC cells from *Hdac11*$^{+/+}$ and *Hdac11*$^{-/-}$ mice were stimulated with 10 MOI of heat-killed *C. albican* (HKCA) or 100 μg/mL zymosan for the indicated time. *Nos2* mRNA levels were measured by quantitative PCR. (C, D) iNOS protein levels. (C) BMDM and (D) BMDC cells from *Hdac11*$^{+/+}$ and *Hdac11*$^{-/-}$ mice were stimulated with 10 MOI HKCA or 100 μg/mL zymosan for 24 h. Cells were lysed by cell lysis buffer with protease inhibitor cocktails, and then the proteins were detected by immunoblotting with an iNOS specific antibody. β-actin was used as loading control. Data in the bar graphs are fold change determinations of target band density in immunoblots. (E, F) NO production. (E) BMDM and (F) BMDC cells from *Hdac11*$^{+/+}$ and *Hdac11*$^{-/-}$ mice were stimulated with 10 MOI of HKCA or 100 μg/mL zymosan for the indicated times. The culture supernatant was collected at the indicated time point and the NO level was measured using Griess regents. (G, H) Fungal killing *in vitro*. (G) BMDM and (H) BMDC cells from *Hdac11*$^{+/+}$ and *Hdac11*$^{-/-}$ were incubated with 1 MOI *C. albicans* for 30 min, and a fungal killing assay was performed 4 h after removal of the unbound particles. (I, J) Phagocytosis efficiency. (I) BMDM and (J) BMDC cells were co-cultured with 1 MOI *C. albicans* for 30 min, then the swallowed fungi particles were compared with the initial infected CFU. Data are shown as the means ± SD, and represent at least three independent experiments. Statistical significance was calculated by One-way ANOVA in (A to F) or Student's *t*-test (G to L). n.s., no significance, *$p < 0.05$, **$p < 0.01$, ***$p < 0.001$.

the potential regulatory role of HDAC11 on *Nos2*/iNOS, we cultured BM-derived macrophages (BMDM) and BM-derived dendritic cells (BMDC) from *Hdac11*$^{+/+}$ or *Hdac11*$^{-/-}$ mice. After exposure to heat-killed *C. albican* (HKCA) or zymosan, a kind of fungi cell wall component, both *Hdac11*$^{-/-}$ BMDM and BMDC cells expressed higher *Nos2* mRNA levels than *Hdac11*$^{+/+}$ cells (Fig. 2A and B). Consistently, iNOS protein levels were also elevated in *Hdac11*$^{-/-}$ BMDM and BMDC cells after HKCA or zymosan treatment (Fig. 2C and D). We also found that various fungal and bacterial stimuli can induce higher *Nos2* and iNOS levels in *Hdac11*$^{-/-}$ BMDM cells (Supplementary Fig. 4D and E). Next, we analyzed the key signaling pathways involved in activating inflammation and fungal infection in BMDM cells treated with HKCA and zymosan. The data showed that loss of *Hdac11* barely affects the MAPKs, NF-κB, and CLR signaling pathways (Supplementary Fig. 4F and G).

As iNOS catalyzes a reaction with arginine to generate NO [33], a biological mediator that can kill invading pathogens, we measured the concentration of NO in cell culture supernatants after treatment with HKCA or zymosan using Griess reagents. We found that *Hdac11*$^{-/-}$ BMDM and BMDC cells produce more NO after HKCA or zymosan treatment compared to *Hdac11*$^{+/+}$ cells (Fig. 2E and F). We also compared the *in vitro* fungal killing efficiencies of *Hdac11*$^{+/+}$ and *Hdac11*$^{-/-}$ cells. Consistent with higher NO levels produced in *Hdac11*$^{-/-}$ cells, *Hdac11*$^{-/-}$ cells could kill *C. albicans* more effectively than *Hdac11*$^{+/+}$ cells, as only half of viable *C. albicans* were detected in *Hdac11*$^{-/-}$ BMDM and BMDC cells (Fig. 2G and H). Other types of peroxides, such as reactive oxygen species (ROS), are important pathogen scavengers [31]. We found that *Hdac11*-deficient BMDM cells produced higher amounts of ROS than *Hdac11*$^{+/+}$ cells upon HKCA or zymosan stimulation (Supplementary Fig. 5A and B). Likewise, pharmacologic inhibition of HDAC11 with inhibitor, FT895, showed a similar ROS production in WT BMDM cells regardless of iNOS activity blockade (Supplementary Fig. 5C and D). Phagocytosis is also a key process in the antifungal response [34]. However, *Hdac11* deletion did not alter phagocytic activity as compared to *Hdac11*$^{+/+}$ cells (Fig. 2J and K). Together, these results show that an *Hdac11* deficiency leads to elevated *Nos2*/iNOS expression and higher NO production after fungal challenge. This mechanism might contribute to the enhanced fungal killing activity observed in *Hdac11*$^{-/-}$ cells.

3.3. Overexpressed HDAC11 inhibits iNOS and fungicidal efficiency

To investigate whether the HDAC11-mediated antifungal response is dependent on its enzyme activity, we constructed an HDAC11 mutant plasmid that contains a dual-site mutant (D181A/H183A) in the zinc-binding domain [25]. Then we introduced Adenovirus (Ad) vectors

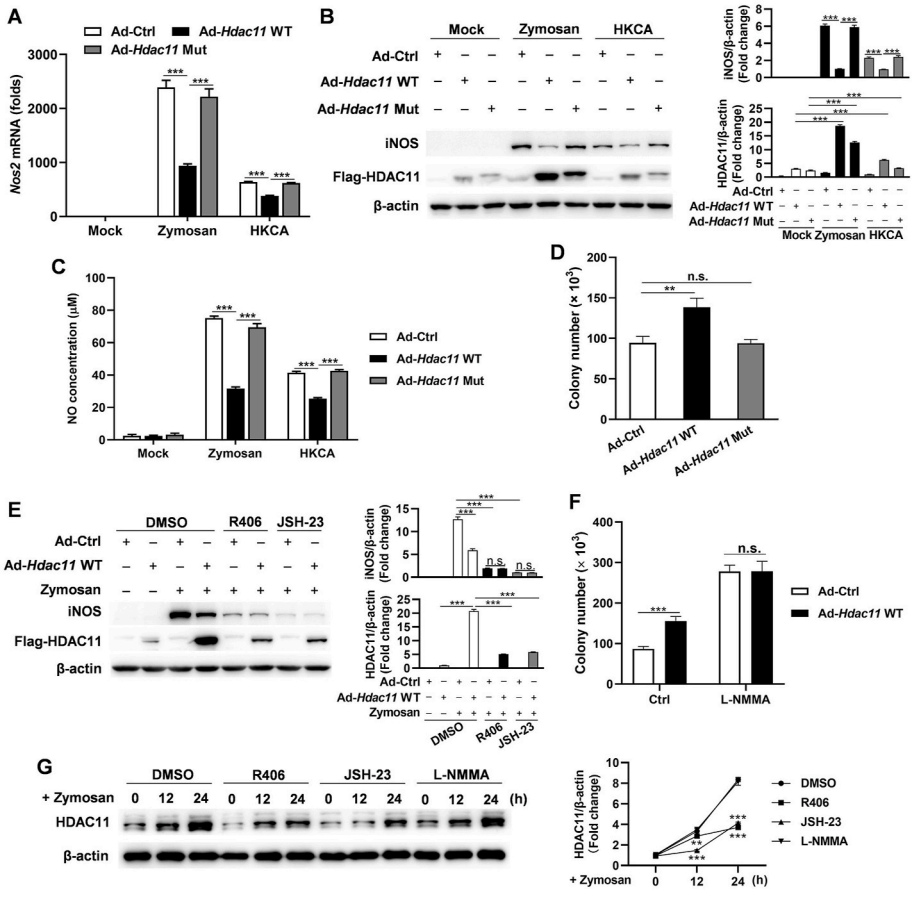

Fig. 3. Overexpression of *Hdac11* decreases NO production and fungal killing activity. (A to C) *Hdac11*$^{-/-}$ BMDM cells were transfected with adenoviruses encoding wild-type *Hdac11* (Ad-*Hdac1*1 WT), catalytically inactive mutant of *Hdac11* (Ad-*Hdac11* Mut), or empty vector as control (Ad-Ctrl) for 48 h. Then the cells were unstimulated (mock) or stimulated with 100 μg/mL zymosan or 10 MOI HKCA for the indicated times. (A) *Nos2* expression. Cells were stimulated for 8 h and then collected for total RNA preparation. *Nos2* mRNA levels were measured by qPCR. (B) iNOS protein levels. After the cells were stimulated for 24 h, total cell protein lysates were performed by SDS-PAGE and immunoblotting with specific antibodies. β-actin was used as a loading control. Data in the bar graphs are fold change determinations of target band density in immunoblots. (C) NO levels. After the cells were stimulated for 48 h, NO production in culture supernatants was measured by Griess regents. (D) Fungal killing activity affected by *Hdac11* overexpression. The fungal killing assay was performed on *Hdac11*$^{-/-}$ BMDM cells 48 h after transfected with Ad-Ctrl, Ad-*Hdac1*1 WT or Ad-*Hdac11* Mut. (E) Expression of iNOS protein after SYK/NF-κB axis blockade. *Hdac11*$^{-/-}$ BMDM cells were transfected with Ad-Ctrl or Ad-*Hdac1*1 WT for 48 h, and treated with 1 μM R406 (SYK inhibitor) or 10 μM JSH-23 (NF-κB inhibitor) for an additional 1 h. DMSO was serves as control. Then these cells were unstimulated or stimulated with 100 μg/mL zymosan for 24 h and total protein lysates were collected for immunoblotting with specific antibodies. β-actin was used as a loading control. Data in the bar graphs are fold change determinations of target band density in immunoblots. (F) Fungal killing activity after iNOS inhibition. *Hdac11*$^{-/-}$ BMDM cells were transfected with Ad-Ctrl or Ad-*Hdac1*1 WT for 48 h, after that cells were untreated or treated with 100 μM L-NMMA (iNOS inhibitor) for an additional 1 h. These cells were then subjected to fungal killing assays. (G) Endogenous HDAC11 protein expression. WT BMDM cells were pre-treated with DMSO control, 1 μM R406, 10 μM JSH-23 or 100 μM L-NMMA for 1 h, and then stimulated with 100 μg/mL zymosan for the indicated times. Total cell protein lysates were performed by SDS-PAGE and immunoblotting with HDAC11 antibody. β-actin was used as a loading control. Data in the line graphs are fold change determinations of target band density in immunoblots. Data are shown as means ± SD, and represent at least three independent experiments. Statistical significance was calculated by One-way ANOVA. n.s., no significance, $^{**}p < 0.01$, $^{***}p < 0.001$.

carrying an RFP control, wild type (WT) or mutant *Hdac11* sequence into BMDM cells before fungi stimuli and determined the *Nos2* and iNOS levels. We found that WT *Hdac11* overexpression significantly inhibited zymosan- or HKCA-triggered *Nos2* and iNOS expression when compared to Ad-control cells, but mutant *Hdac11* lost the effect (Fig. 3A and B). Consistently, WT *Hdac11* overexpression also reduced NO production after zymosan or HKCA treatment, but mutant *Hdac11* did not (Fig. 3C). We also observed reduced fungicidal efficiency in WT *Hdac11* overexpressing cells, but not mutant *Hdac11* cells, as compared to control cells (Fig. 3D). These results suggest that HDAC11 inhibits iNOS levels, and thus fungicidal efficiency, depending on its enzymatic activity.

Next, we want to explore how HDAC11 and HDAC11-mediated antifungal activity are regulated after infection. Pharmacologic inhibition of SYK and NF-κB using R406 and JSH-23, respectively, abrogated iNOS expression in BMDM cells triggered by zymosan (Fig. 3E). Meanwhile, the trend toward increased expression of exogenous HDAC11 was also suppressed by SYK or NF-κB inhibition (Fig. 3E). Furthermore, we performed the fungal killing assay in Ad-mediated exogenous HDAC11-expressing BMDM cells. We found that the effect of reduced fungicidal activity in HDAC11-overexpressing BMDM cells was abolished in the presences of the iNOS inhibitor L-NMMA (Fig. 3F). In addition, treatment with zymosan highly induced endogenous HDAC11 in BMDM cells, and the effect could be abrogated when SYK or NF-κB but not iNOS activity was pharmacologically inhibited (Fig. 3G). Thus, these data suggest that HDAC11 is induced in phagocytes in response to fungal infection that is dependent on SYK/NF-κB signaling, at least in part.

3.4. HDAC11 negatively regulates Nos2 expression through chromatin modification

We next investigated the mechanisms by which *Hdac11* deficiency leads to enhanced *Nos2* expression after fungal infection. To gain insight into the potential chromatin modifications induced by HDAC11, we treated *Hdac11*$^{+/+}$ and *Hdac11*$^{-/-}$ BMDM cells with zymosan for 1 h, and then evaluated the histone H3 and H4 changes in the proximal (−145 to −38) and distal (−1146 to −1034) regions of the *Nos2* promoter by ChIP analysis. The ChIP data showed that more histone H3 acetylation in both proximal and distal regions of the *Nos2* promoter in *Hdac11*$^{-/-}$ cells compared to *Hdac11*$^{+/+}$ cells (Fig. 4A). *Hdac11* loss also increased histone H4 acetylation at *Nos2* promoter (Fig. 4B). Strikingly, we observed a lower degree of H4 acetylation in the distal region than in the proximal region (Fig. 4B) for unknown reasons.

Signal transducers and activators of transcription 3 (STAT3), is a *Nos2* transcriptional repressor [35]. STAT3 binding to the *Nos2* promoter was significantly reduced in *Hdac11*$^{-/-}$ BMDM cells after zymosan stimulation (Fig. 4C). We further determined whether other molecules involved in the STAT3 pathway bind the *Nos2* promoter, such as transcription factor EB (TFEB) [36] and protein inhibitor of activated STAT1 (PIAS1) [37]. ChIP analysis confirmed that TFEB can bind to *Nos2* promoter but PIAS1 not, however, there was no significant difference between *Hdac11*$^{+/+}$ and *Hdac11*$^{-/-}$ cells after stimulated with zymosan (Fig. 4D and E). Furthermore, we evaluated the effect of HDAC11 deficiency on *Nos2* transcriptional activity by determining the level of RNA polymerase II (pol II) binding to the *Nos2* promoter. *Hdac11*$^{-/-}$ cells stimulated with fungi components showed an increase

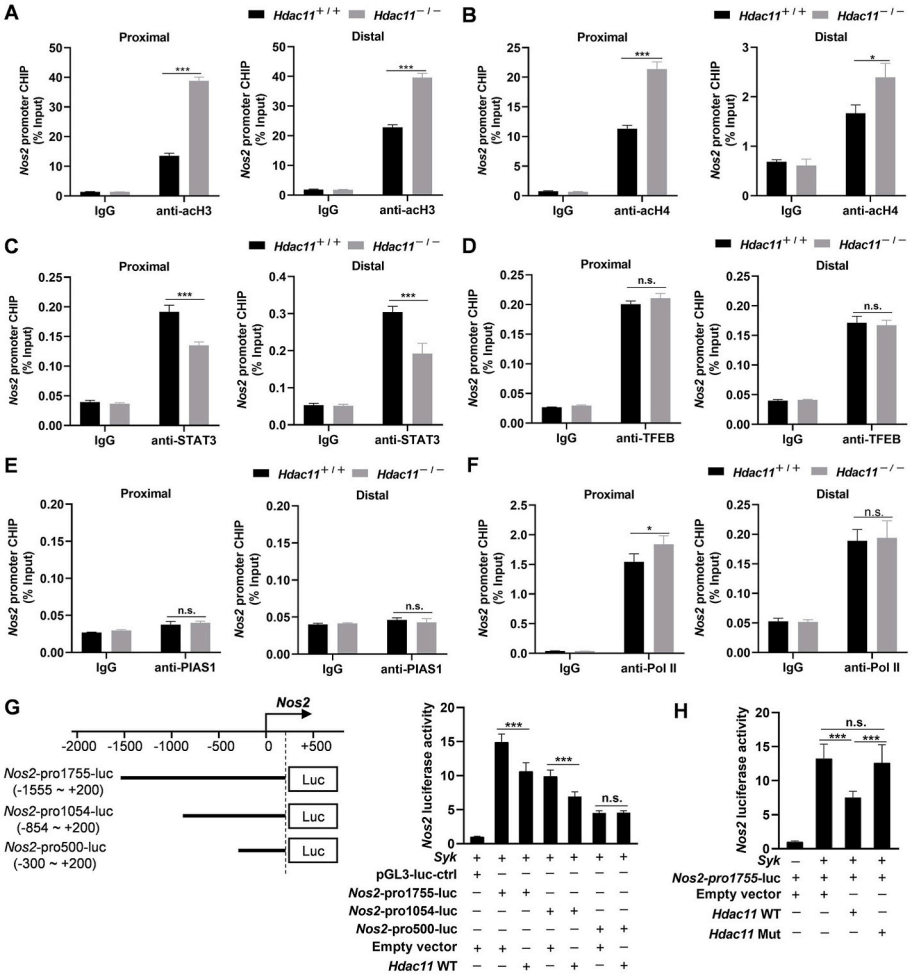

Fig. 4. *Hdac11* negatively regulates *Nos2* expression through chromatin modification. (A to F) BMDM cells from *Hdac11*$^{+/+}$ and *Hdac11*$^{-/-}$ mice were stimulated with 100 μg/mL of zymosan for 1 h. ChIP analysis were performed with (A) anti-acetylated histone 3 (acH3), (B) anti-acetylated histone 4 (acH4), (C) anti-STAT3, (D) anti-TFEB, (E) anti-PIAS1, and (F) anti-RNA polymerase II (Pol II) antibodies, and normal rabbit IgG was served as negative control. Then the binding genome DNA were purified and different regions of the *Nos2* gene promoter, including proximal (−145 to −38) and distal (−1146 to −1034) positions, were measured by qPCR. Data are presented as the percentage of input before immunoprecipitation. The data are representative of two independent experiments with similar results. (G and H) Luciferase activity assay of *Nos2* promoter reporter gene. (G) HEK293T cells were transfected with constructs of deletion mutants of the *Nos2* gene promoter *Nos2*-pro1755-luc (−1555 to +200) or *Nos2*-pro1054-luc (−854 to +200) or *Nos2*-pro500-luc (−300 to +200), and *Hdac1*1 WT plasmid as indicated for 24 h. (H) HEK293T cells transfected with empty vector or *Hdac1*1 WT or *Hdac11* Mut plasmids and *Nos2*-pro1755-luc as indicated for 24 h. Luciferase assays were performed and the luciferase activity was normalized to *Renilla* luciferase. Data are shown as means ± SD. Data are representative of at least three independent experiments unless stated otherwise. Statistical significance was calculated by One-way ANOVA. n.s., no significance, *$p < 0.05$, ***$p < 0.001$.

in pol II binding in the proximal but not the distal regions of the *Nos2* promoter (Fig. 4F). In addition, *Nos2* promoter deletion assays showed that the decreased activity was abolished in pro500-luc (−300 to +200), but neither pro1054-luc (−854 to +200) nor pro1755-luc (−1555 to +200) plasmid co-transfected HDAC11 overexpressing cells, indicating that HDAC11 binds to *Nos2* promoter at the region of −854 to −300 (position relative to the transcription start site) (Fig. 4G). Moreover, we confirmed that mutant *Hdac11* can restore the inhibitory effect of WT *Hdac11* on *Nos2* gene luciferase activity as compared to empty vector-transfected cells (Fig. 4H). Collectively, these results indicate that HDAC11 negatively regulates *Nos2* expression through chromatin modification.

3.5. STAT3 is a transcriptional repressor for Nos2 promoter

Several transcription factors, including STAT3, IRF1, and Smad3, are known to be involved in *Nos2* gene transcriptional regulation [35,38,39]. Thus, we want to know whether STAT3 and HDAC11 regulate *Nos2* promoter transcription activity as part of complex. Indeed, we found by overexpression assays that only STAT3 can interact with HDAC11 (Fig. 5A, and Supplementary Fig. 6, A to C). We also confirmed the endogenous interaction between HDAC11 and STAT3 in zymosan-activated BMDM cells (Fig. 5B). To further investigate the molecular mechanisms of STAT3 in HDAC11-mediated *Nos2* transcriptional regulation, we treated WT BMDM cells with zymosan in the absence or presence of the STAT3 specific inhibitor, STAT3-IN-1, and then determined the transcriptional activity of the *Nos2* promoter by ChIP. STAT3-IN-1 pre-treated cells exhibited lower abundances of STAT3 binding at the *Nos2* promoter in both proximal and distal positions than control cells (Fig. 5C). In the STAT3-IN-1 treated cells, HDAC11 enrichment in the proximal region was markedly reduced, while in the distal region was almost undetectable (Fig. 5D). The binding efficiency of pol II to the *Nos2* promoter after STAT3 inhibition was similar to that in *Hdac11*-deficient cells, with an increasing in the proximal but no difference in the distal region (Fig. 5E). These results suggest that STAT3 is involved in HDAC11-mediated *Nos2* regulation.

Next, we determined the mRNA levels of pro-inflammatory cytokines in BMDM cells stimulated by zymosan following pharmacological inhibition of STAT3. We observed that STAT3 inhibition upregulated *Nos2* expression but downregulated *Il1b* and *Il6* (Supplementary Fig. 6D). Moreover, luciferase activity driven by the *Nos2* promoter was significantly reduced in STAT3 overexpressing cells when compared to empty vector-transfected cells; however, the reduction effect was abolished by STAT3-IN-1 (Fig. 5F). We also co-transfected HDAC11 and STAT3 into HEK-293T cells expressing *Nos2* promoter-derived luciferase and determined the rescue effect by inhibiting HDAC11 or STAT3 alone. We found that the HDAC11 inhibitor FT895 almost completely rescued the inhibition of luciferase activity co-transfected with HDAC11 and STAT3,

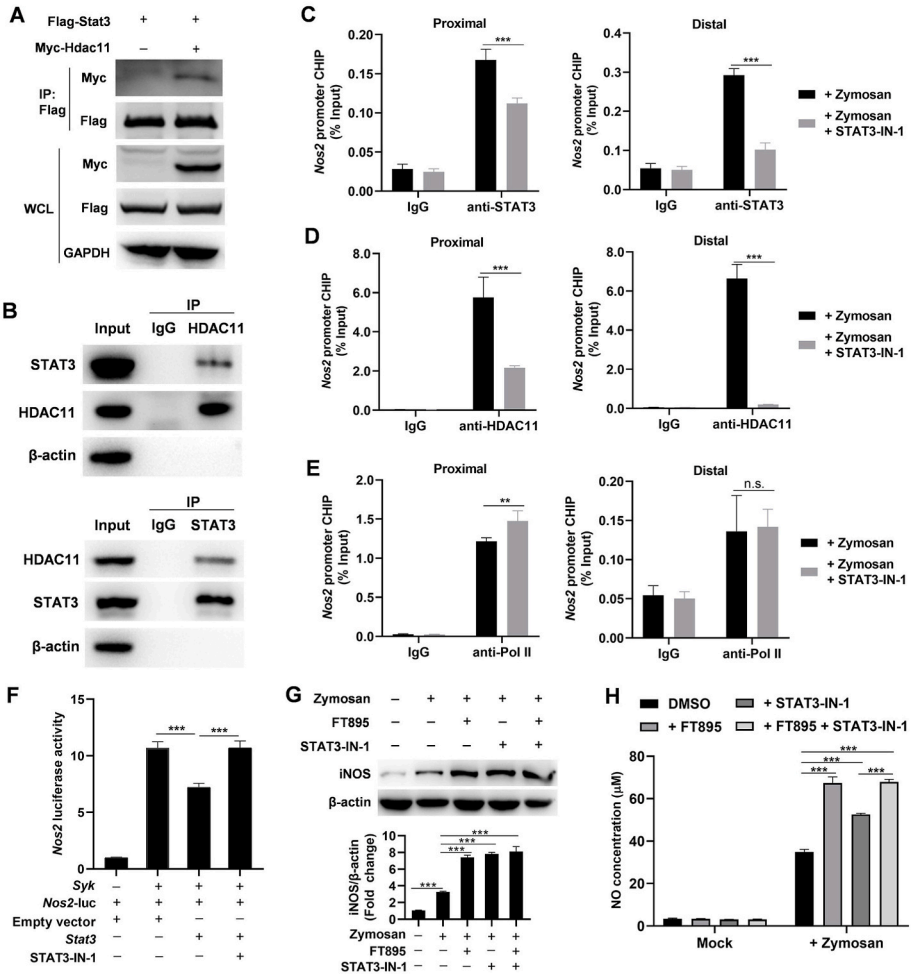

Fig. 5. STAT3 interacts with HDAC11 and participates in *Nos2* repression. (A) HDAC11 associates with STAT3. HEK293T cells were transfected with plasmids encoding Flag-*Stat3* and Myc-*Hdac11* for 24 h. Immunoblot analysis of Myc-HDAC11 immunoprecipitated with antibodies to Flag tags. (B) Interaction of endogenous HDAC11 with STAT3 in BMDM cells. BMDM cells were stimulated with 100 μg/mL zymosan for 1 h. Immunoblot analysis of endogenous STAT3 or HDAC11 immunoprecipitated with antibody to HDAC11 (upper panels) and STAT3 (lower panels). IgG was used as control. (C to E) WT BMDM cells were pre-treated with or without STAT3 inhibitor, STAT3-IN-1, for 30 min, then stimulated with 100 μg/mL zymosan for another 1 h. ChIP analysis was performed with (A) anti-STAT3, (B) anti-HDAC11, and (C) anti-Pol II antibodies, and normal IgG (as a negative control). The enrichments of DNA at the proximal and distal positions of the *Nos2* gene promoter were measured by qPCR. Data are presented as the percentage of input before immunoprecipitation. The data are representative of two independent experiments with similar results. (F) Luciferase activity assay of the *Nos2* promoter reporter activated by Syk in lysates of HEK293T cells transfected with empty vector, *Hdac1*1 WT or *Hdac11* Mut plasmids as indicated. (G) iNOS proteins. WT BMDM cells were unstimulated or stimulated with 100 μg/mL zymosan for 24 h in the presence of FT895 or STAT3-IN-1 alone, or FT895 and STAT3-IN-1 in combination. Cell lysates were performed for immunoblotting with iNOS antibody. β-actin was used as a loading control. Data in the bar graphs are fold change determinations of target band density in immunoblots. (H) NO production. WT BMDM cells were unstimulated or stimulated with 100 μg/mL zymosan in the presence of FT895 or STAT3-IN-1 alone, or FT895 and STAT3-IN-1 in combination for 48 h. NO levels in culture supernatants were measured by nitrite assay. Data are shown as means ± SD. The data are representative of at least three independent experiments unless stated otherwise. Statistical significance was calculated by One-way ANOVA. n.s., no significance, $^{**}p < 0.01$, $^{***}p < 0.001$.

however, the extent was relatively lower in STAT3-IN-1 treated cells (Supplementary Fig. 6E). We next wanted to determine whether the combined inhibition of HDAC11 and STAT3 promotes iNOS expression and NO production better than either single treatment. In zymosan-stimulated BMDM cells, iNOS levels were elevated in cells with these inhibitors treated alone or in combination (Fig. 5G). Unexpectedly, after zymosan stimulation, BMDM cells treated with a combination of STAT3 and HDAC11 inhibitors showed comparable levels of iNOS expression compared to cells treated with either STAT3 or HDAC11 inhibitor alone (Fig. 5G). Compared to the cells treated with FT895 and STAT3-IN-1 in combination, the level of NO production was comparable in FT895-treated cells, but relatively lower in STAT3-IN-1-treated cells (Fig. 5H). Taken together, these results suggest that HDAC11 and STAT3 can jointly repress *Nos2* gene transcription.

Acetylation and phosphorylation are crucial posttranslational modifications that regulate the activities of numerous proteins, including STATs [40]. A previous study found that the class I HDAC, HDAC3, physically interacts with STAT3 and affects STAT3 acetylation and phosphorylation in B cells [41]. We thus finally determined the effect of HDAC11 on STAT3 acetylation and phosphorylation. Unlike HDAC3, HDAC11 deficiency slightly lowered $STAT3^{Ser727}$ phosphorylation but barely affected acetylation (Supplementary Fig. 6F), suggesting a different mechanism of action.

3.6. iNOS enhances antifungal responses in the absence of HDAC11

To confirm the role of iNOS in *Hdac11*-deficienct mice in response to fungal infection, we treated *C.albicans* infected *Hdac11*$^{-/-}$ mice with the iNOS specific inhibitor SMT. SMT significantly reduced the survival rate and weight of these mice as compared with the control treatment (Fig. 6A and B). Furthermore, the fungal titer in kidneys of mice treated with SMT was significantly increased compared to control mice (Fig. 6C). As confirmation, another NOS inhibitor, L-NMMA, also reduced the survival rate and weight of infected *Hdac11*$^{-/-}$ mice (Fig. 6D and E), and increased the fungal titer in the kidney (Fig. 6F). Histopathologic analysis of kidneys of infected mice showed that both SMT and L-NMMA treatment increased renal inflammation and fungi invasion (Fig. 6G and H). As expected, the protein levels of iNOS were

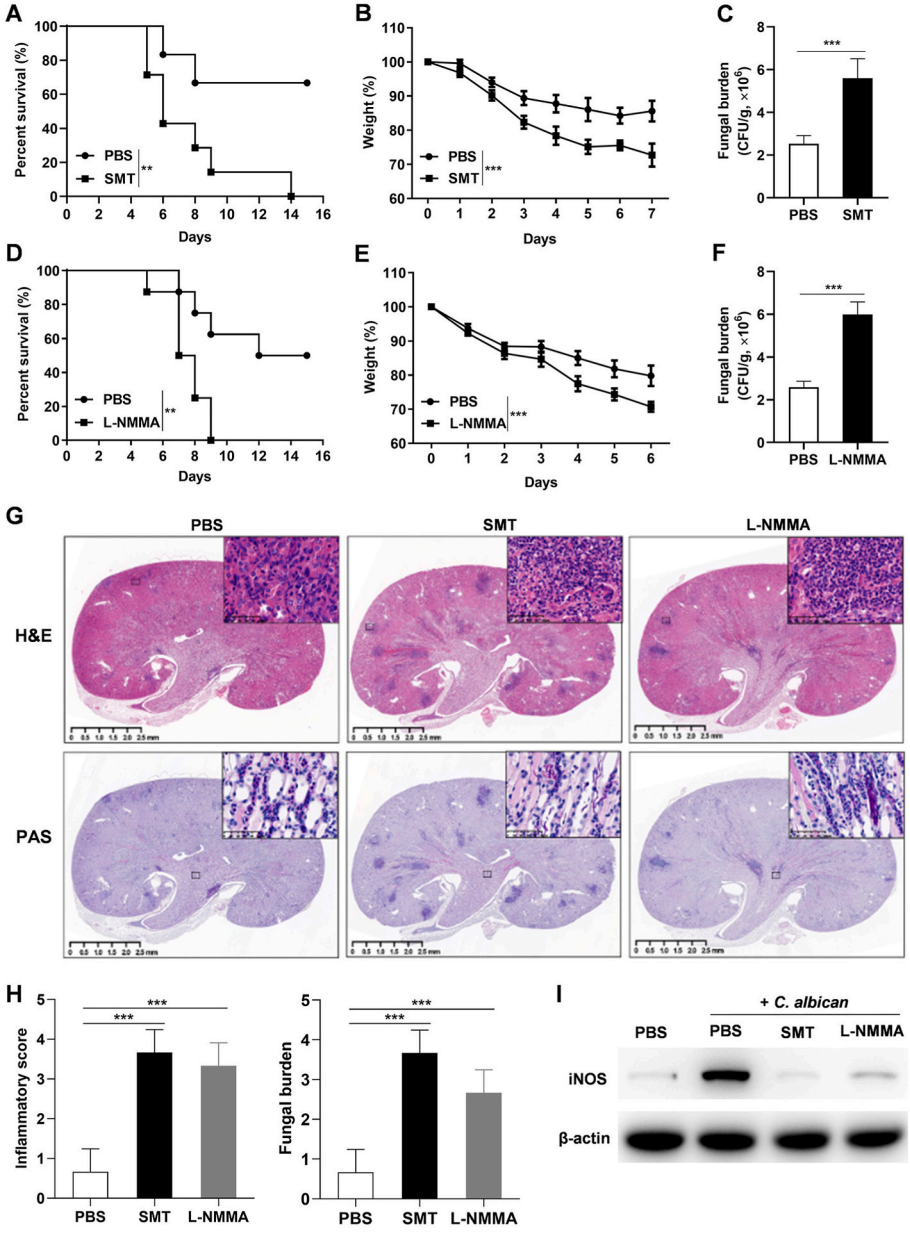

Fig. 6. iNOS expression in *Hdac11* deficient mice is responsible for host antifungal immune response. (A, B) *Hdac11*$^{-/-}$ mice were intravenously infected with 1×10^5 CFU of *C. albicans* per mouse. Infected mice were intraperitonially administered with iNOS inhibitor SMT in a dose of 50 mg/kg body weight (n = 7) or PBS (n = 6) daily for 4 consecutive days. (A) Mouse survival and (B) weight were monitored after infection. (C) *Hdac11*$^{-/-}$ mice were intravenously injected with 200 μl PBS containing 2×10^5 CFU of *C. albicans* and iNOS inhibitor SMT (50 mg/kg body weigh) or *C. albicans* only for each mouse (n = 3 mice for each group). Mice kidneys were isolated 48 h after infection and fungal burden was measured on YPD plates. (D, E) *Hdac11*$^{-/-}$ mice were infected intravenously with 1×10^5 CFU of *C. albicans* per mouse. Infected mice (n = 8 mice for each group) were intraperitoneally administered total NOS inhibitor L-NMMA (100 mg/kg body weight) or PBS daily for 4 consecutive days. (D) Mouse survival and (E) weight were monitored after infection. (F) *Hdac11*$^{-/-}$ mice were intravenously injected with 200 μl PBS containing 2×10^5 CFU of *C. albicans* and L-NMMA (100 mg/kg body weigh) or *C. albican* only for each mouse (n = 3 mice for each group). Kidney fungal burden was measured 48 h after infection as in (C). (G) *Hdac11*$^{-/-}$ mice infected with 200 μl PBS containing 2×10^5 CFU of *C. albicans* alone, or together with SMT (50 mg/kg body weigh) or L-NMMA (100 mg/kg body weigh) for 48 h (n = 3 for each group). Kidney sections from these mice were stained with H&E (upper panels) and PAS (lower panels). Insets show regions of inflammation or fungal growth. Representative images of at least three replicates are shown. Scale bar, 500 μm. (H) The inflammatory score (left panel) based on renal immune cell infiltration/inflammation and tissue destruction, and the fungal burden (right panel) are shown. At least three mice for each group and three sections per kidney were analyzed. (I) iNOS induction. *Hdac11*$^{-/-}$ mice were uninfected or infected with *C. albicans* as seen in (G). Total renal protein lysates immunoblotted with iNOS specific antibody. β-actin was used as a loading control. Data are shown as means ± SD. Data are representative of at least two independent experiments with similar results. Statistical significance for survival was assessed by log rank test and for weight change by two-way ANOVA. A two-tailed unpaired *t*-test was performed between only two groups. $^{**}p < 0.01$, $^{***}p < 0.001$.

remarkably reduced in the kidneys from *C.albicans*-infected *Hdac11*$^{-/-}$ mice folloing SMT and L-NMMA administration compared to control treatment (Fig. 6I). These data suggest that iNOS-mediated effects enhance antifungal responses in *Hdac11*-deficienct mice.

3.7. The HDAC11 inhibitor FT895 shows potential therapeutic effects for fungal infection

Various HDAC11 inhibitors have been designed, such as FT895 and SIS17 [42,43], which inactivate deacetylase as well as defatty-acylase activities. To investigate whether these HDAC11 inhibitors can effectively promote the antifungal responses, we infected WT mice with *C. albicans* and then treated them with the HDAC11 inhibitor FT895 or SIS17. Treatment with FT895, but not SIS17, increased the survival rate and ameliorated the weight loss compared to mice given DMSO alone (Fig. 7A and B). In addition, FT895 also significantly reduced the fungal burden in the kidney, while SIS17 did not (Fig. 7C). As SIS17 was screened for its inhibitory effect on the defatty-acylation activity of HDAC11, this finding suggests that HDAC11-mediated antifungal responses are independent of the biological role of defatty acylation. Furthermore, FT895 effectively diminished the pathological damage and fungal invasion in the kidney after fungal infection *in vivo* (Fig. 7D and E). To confirm the antifungal effect of the HDAC11 inhibitor FT895 *in vitro*, we pretreated BMDM cells with FT895 and then stimulated them

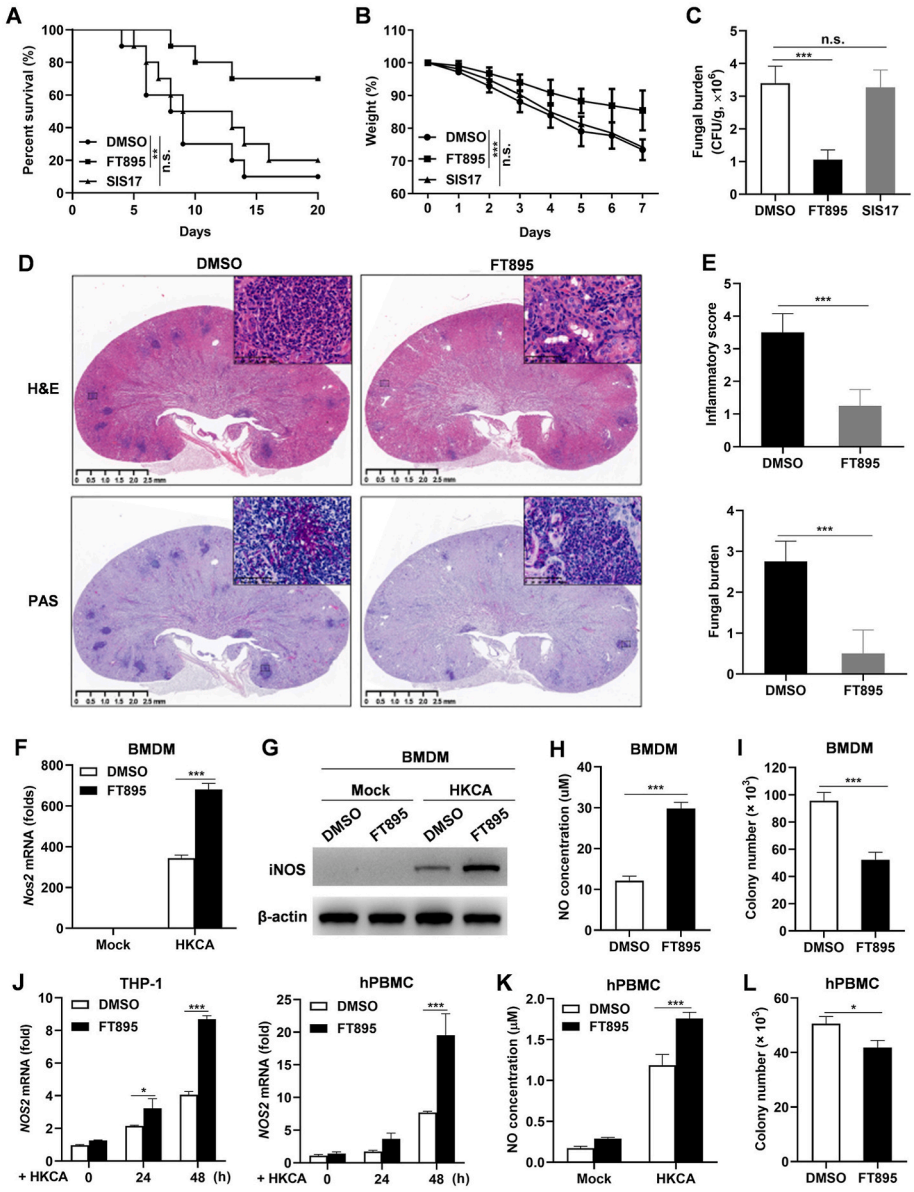

Fig. 7. HDAC11 inhibitor FT895 shows potential therapeutic effect in fungal infection. (A, B) WT C57BL/6 mice were intravenously injected with 2 × 10^5 CFU of *C. albicans* per mouse, then randomly divided into three groups (n = 10 mice for each group) and 24 h later intraperitoneally administered with HDAC11 inhibitors FT895 (50 mg/kg body weight) or SIS17 (100 mg/kg body weight) or equal volume of DMSO as control per day for 4 consecutive days. (A) Mouse survival rate and (B) weight change were monitored after infection. (C) Kidney fungal burden. WT mice were infected intravenously with 2 × 10^5 CFU of *C. albicans* per mouse, and 24 h later treated with DMSO, FT895, or SIS17 (n = 3 mice for each group). After an additional 48 h, the kidneys were isolated and the fungal burden was determined by YPD plate assay. (D) Kidney sections from DMSO or HDAC11 inhibitor FT895 treated mice infected *C. albicans* as in (C) were stained with H&E and PAS. Insets show regions of inflammation and fungal growth, respectively. Representative images of at least three replicates are shown. Scale bar, 500 μm. (E) The inflammatory score and the fungal burden based on the kidney stains in (D) are shown. At least three mice for each group and three sections per kidney were analyzed. (F) *Nos2* levels in mouse BMDM cells. WT mouse BMDM cells were mock infected or infected with HKCA (MOI = 10) in the absence or presence of FT895 (10 μM). After 8 h, the cells were collected for total preparation. *Nos2* mRNA levels were measured by qPCR. (G) iNOS expression. BMDM cells were treated as in (D). After 24 h, the cell lysates were collected and immunoblotting with iNOS antibody. β-actin was used as a loading control. (H) NO production in mouse BMDM cells. WT mouse BMDM cells were treated as in (D). Culture supernatants were collected 48 h later and measured for NO production by nitrite assay. (I) Fungal killing efficiency of mouse BMDM cells. A fungal killing assay was performed on BMDM cells pretreated with 10 μM FT895 or DMSO as control for 1 h. (J) *NOS2* mRNA triggered in human cells. Human monocyte cell line THP-1 (left panel) and primary peripheral blood mononuclear cells (hPBMC, right panel) were stimulated with 10 MOI of HKCA for the indicated times in the presence of FT895 (10 μM) or DMSO as control. Total RNA was extracted and *NOS2* mRNA levels were measured by qPCR. β-actin house keep gene was used as reference. (K) NO production in hPBMC. hPBMC were pretreated with FT895 (10 μM) or DMSO for 1 h, and then stimulated with HKCA (10 MOI) for an additional 48 h. NO levels in culture supernatants were determined as in (H). (L) Fungal killing activity of hPBMC. Fungal killing assay was performed on PBMC cells pretreated with 10 μM FT895 or DMSO as control for 1 h. The data are shown as means ± SD. Data are representative of three independent experiments. Statistical significance for survival was assessed by log rank test and for weight change by two-way ANOVA. A two-tailed unpaired *t*-test was performed between only two groups. n.s., no significance, $^*p < 0.05$, $^{**}p < 0.01$, $^{***}p < 0.001$.

with HKCA. Quantitative PCR and immunoblot analysis showed higher *Nos2* and iNOS expression in FT895-treated cells than DMSO-treated cells (Fig. 7F and G). Consistently, FT895 treated BMDM cells produced more NO triggered by HKCA than control cells (Fig. 7H). An *in vitro* fungal killing assay showed that FT895 enhanced the fungicidal efficiency of BMDM cells (Fig. 7I). Collectively, these data demonstrate that HDAC11 specific inhibitor FT895 can promote antifungal responses.

To further test the relevance of the findings made in mice to human diseases, we infected the PMA-induced human monocyte macrophages cell line THP-1 and human peripheral blood mononuclear cells (hPBMC) with HKCA. THP-1 cells treated with FT895 showed significant upregulation of *Nos2* mRNA levels (Fig. 7J). Similarly, FT895 also boosted *Nos2* levels at the mRNA in hPBMC triggered by HKCA (Fig. 7J). Moreover, hPBMC treated with FT895 produced more NO and killed fungi more efficiently (Fig. 7K and L). Thus, inhibiting HDAC11 by FT895 showed beneficial effects in human cells when challenged with fungal infection.

In summary, we have conclude that after infection, *C. albicans* is sensed by the CLR, such as Dectin-1, which activates SYK/NF-κB signaling and further induces the expression of *Nos2* and NO production, functioning as a fungal killing mediator. Moreover, the SYK/NF-κB signaling also increases HDAC11 expression, at least in part, which can interact with STAT3 and jointly repress *Nos2* transcription. In the absence of HDAC11, the transcriptional repression of *Nos2* is relieved, thereby promoting NO production and fungicidal activity (Fig. 8). Therefore, HDAC11 may serve as a potential therapeutic target of clinical *C.albicans* infection, as HDAC11 inhibition enhances antifungal immunity.

4. Discussion

In the current study, we have demonstrated that HDAC11 plays a crucial role in regulating innate immune responses against fungal infection. Specifically, we found that *Hdac11*$^{-/-}$ mice are more resistant to *C. albicans* infection than WT mice, and *Hdac11* deficiency in phagocytes is vital for this protective effect. Moreover, adaptive transplantation of macrophages from *Hdac11*$^{-/-}$ mice into WT mice with macrophage deletion *in vivo* significantly reduces the fungal burden in renal tissue when compared to WT macrophage transplantation, suggesting an enhanced innate immune response against fungal infection in *Hdac11* deficient mice. HDAC11 inhibition shows a beneficial antifungal effect, both *in vitro* and *in vivo*, through upregulating *Nos2*/iNOS expression and NO production. Mechanistically, *Hdac11* inhibition leads to elevated *Nos2* gene expression through chromatin modification and a much higher level of NO production that kills fungi. Notably, STAT3, a transcriptional repressor of *Nos2* promoter, physically interacts with HDAC11 and is tightly involved in HDAC11-mediated *Nos2* regulation.

The functions of HDAC11 in innate and adaptive immune cells have been extensively studied by using deficient mice [16,21,23,24,44]. Recently, there has been increasing interests in the role of HDAC11 in regulating pro-inflammatory and anti-inflammatory effects in different immune cells. In macrophages, HDAC11 is a negative regulator of the anti-inflammatory cytokine IL-10, and HDAC11 knockdown cells manifest immune tolerance phenotype [23]. Myeloid-derived suppressor cells (MDSCs) lacking HDAC11 displayed an increased suppressive activity against CD8^{+} T-cells [44]. Conversely, deletion of HDAC11 in T cells promotes pro-inflammatory Th1 cell differentiation and enhanced effector T cell responses [24]. In the absence of HDAC11, neutrophils also become more inflammatory with higher expression of TNF-α and IL-6 [21]. Together with the work we present here, we can conclude that HDAC11 is a multifaceted immunomodulator in innate and adaptive immune cells, and its function may differ depending on the cell type or microenvironments the cell locates. The functional role of HDAC11 in host defense against invaded pathogens, especially the *C. albican*, had not been well studied prior to this work. We now know that HDAC11 is a negative modulator for the host innate response to fungal infection. More importantly, our findings suggest a potential approach to treating the fungal infection with an HDAC11 inhibitor.

During fungal infection, phagocytes have a marked influence on the inflammatory environment by the expression of various pro-inflammatory cytokines, chemokines, and other mediators, such as NO and ROS [31]. Data from a recent study showed that CD23 activation-induced iNOS expression after *C. albicans* infection is responsible for fungi pathogens clearance by macrophages and DCs [23], which highlights the importance of NO production in antifungal immunity. Our data shows that genetic deletion or pharmacological inhibition of HDAC11 leads to more NO and ROS production, and enhanced fungicidal activity of phagocytes. However, HDAC11 deficiency decreased the levels of pro-inflammatory cytokines IL-1β and IL-6 after systemic *C. albicans* infection. The reduction of IL-1β and IL-6 does not coincide with the enhanced antifungal immunity in HDAC11 deficient mice. This may be an indirect consequence of reduced fungal invasion as higher NO production and enhanced fungal killing by HDAC11 deficient mice. Many mechanisms are involved in regulating host antifungal immune responses, such as CLR, NF-κB, and MAPKs signaling pathways [3]; however, these pathways were barely affected in phagocytes lacking HDAC11. Strikingly, HDAC11 protein levels were

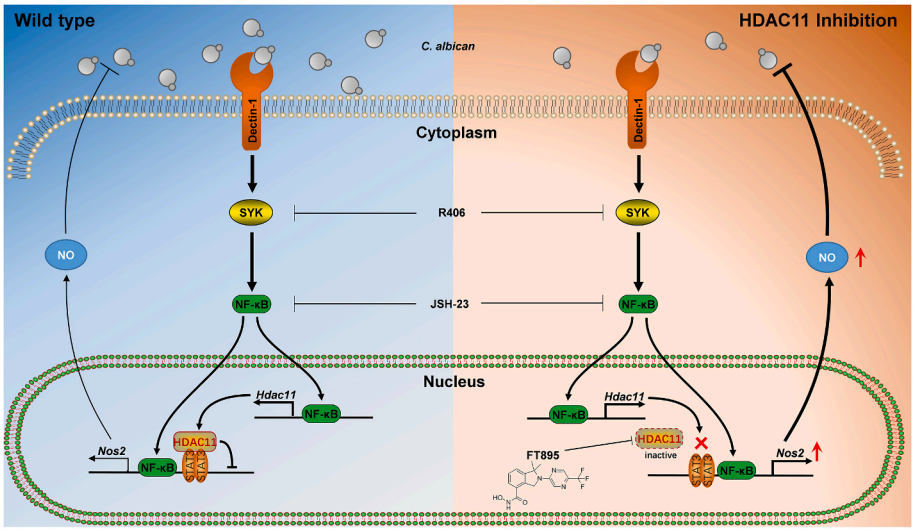

Fig. 8. HDAC11 inhibition enhances the antifungal response in macrophages. Proposed working model for the mechanism by which HDAC11 regulates the antifungal immunity. Upon infection, *C. albicans* are sensed by the CLR, such as Dectin-1, which can activate SYK/NF-κB signaling and initiate *Nos2* transcription. On the other hand, HDAC11 can also be induced, at least in part, in an NF-κB-dependent manner. HDAC11 can interact with STAT3 and jointly repress *Nos2* transcription. However, in HDAC11-inactivated cells, the transcriptional repression of *Nos2* is relieved, which in turn enhances the production of NO and fungicidal activity.

increased in macrophages following treatment with fungal ligands, and SYK/NF-κB signaling inhibition could abolish the increase of HDAC11, suggesting an NF-κB-dependent manner, at least in part, for HDAC11 induction during fungal infection. Based on our observations, we speculate that SYK activation-dependent HDAC11 upregulation in host cells is a response to fungal infection, which may be involved in the fine regulation of antifungal immunity. In a recent study, cigarette smoke extract was found to promote HDAC11 degradation in lung epithelial cells through poly-ubiquitination of lysine (Lys) residues at Lys50 and Lys280 positions [45]. Although the poly-ubiquitination lysine sites in HDAC11 protein have been characterized, the E3 ubiquitin ligase associated with HDAC11 remains to be identified and warrants further investigation.

HDACs do not directly bind to DNA and they perform their functions as part of multiprotein complexes that can associate to target gene promoters [46]. In our study, we reported that STAT3, a transcriptional repressor of *Nos2* gene, physically interacts with HDAC11, and functions as a scaffold protein supporting HDAC11 association with *Nos2* promoter. STAT3 inhibition markedly reduced HDAC11 enrichment at the *Nos2* promoter, especially in the distal region. Similarly, HDAC11 deletion also lowered the abundance of STAT3 binding at the *Nos2* promoter. These observations suggest that STAT3 plays a vital role in HDAC11-mediated *Nos2* suppression. Accordingly, a recent study evidenced that STAT3 represses *NOS2* expression in human macrophages upon *mycobacterium tuberculosis* infection [47]. STAT3 undergoes a variety of posttranslational modifications, including acetylation and phosphorylation, which can affect its dimerization, activation, and nuclear translocation [48]. There is increasing evidence indicating that multiple HDACs interact with STAT3 and change its modifications. For instance, HDAC1 or HDAC3 knockdown upregulated STAT3 acetylation and promoted accumulation in the nucleus [41,49]. However, we found that loss of HDAC11 resulted in decreased STAT3 phosphorylation but no change in acetylation, suggesting a different regulatory mechanism for STAT3 signaling. These findings might help extend the exploration of the biological functions of HDACs involved in physiological and pathological processes.

In summary, we provide new insights into the negative regulation of antifungal immunity. HDAC11 functions in phagocytes by interacting with the transcriptional repressor STAT3 to regulate *Nos2* expression through chromatin modification. We show for the first time that selective HDAC inhibition might be a suitable approach for the treatment of *C. albicans* infection *in vitro* and *in vivo*.

Author contributions

WLC and HW designed the research and wrote the manuscript. HW and XFY conducted most of the experiments and interpreted data. XBZ performed bone marrow transplantation and systemic infection experiments. ZRW and HMT performed flow cytometry analysis. YX and JZQ helped ChIP experiments. QQD helped with ELISA experiments. PS provided Hdac11 knockout mice. All authors reviewed the manuscript.

Declaration of competing interest

The authors have declared no conflict of interest in this work.

Acknowledgments

This work was supported by grants from the National Natural Science Foundation of China (31870908, U1801283), grants from the Shenzhen Science and Technology Innovation Commission (JCYJ20210324094611031, JCYJ20180507182253653), the Guangdong Provincial Science and Technology Program (2019B030301009, 2019A1515110718). We thank Jessica Kate Tamanini (Scientific Editor, Shenzhen University School of Medicine) for editing manuscript.

Appendix A. Supplementary data

Supplementary data to this article can be found online at https://doi.org/10.1016/j.redox.2022.102461.

References

[1] G.D. Brown, D.W. Denning, N.A. Gow, S.M. Levitz, M.G. Netea, T.C. White, Hidden killers: human fungal infections, Sci. Transl. Med. 4 (2012) 165rv113.
[2] J.Y. Kim, Human fungal pathogens: why should we learn? J. Microbiol. 54 (2016) 145–148.
[3] M.G. Netea, L.A. Joosten, J.W. van der Meer, B.J. Kullberg, F.L. van de Veerdonk, Immune defence against Candida fungal infections, Nature reviews, Immunology 15 (2015) 630–642.
[4] Y. Lee, E. Puumala, N. Robbins, L.E. Cowen, Antifungal drug resistance: molecular mechanisms in Candida albicans and beyond, Chem. Rev. 121 (2021) 3390–3411.
[5] A. Plato, S.E. Hardison, G.D. Brown, Pattern recognition receptors in antifungal immunity, Semin. Immunopathol. 37 (2015) 97–106.
[6] S. Yamasaki, M. Matsumoto, O. Takeuchi, T. Matsuzawa, E. Ishikawa, M. Sakuma, H. Tateno, J. Uno, J. Hirabayashi, Y. Mikami, K. Takeda, S. Akira, T. Saito, C-type lectin Mincle is an activating receptor for pathogenic fungus, Malassezia, Proc. Natl. Acad. Sci. U.S.A. 106 (2009) 1897–1902.
[7] S. Saijo, S. Ikeda, K. Yamabe, S. Kakuta, H. Ishigame, A. Akitsu, N. Fujikado, T. Kusaka, S. Kubo, S.H. Chung, R. Komatsu, N. Miura, Y. Adachi, N. Ohno, K. Shibuya, N. Yamamoto, K. Kawakami, S. Yamasaki, T. Saito, S. Akira, Y. Iwakura, Dectin-2 recognition of alpha-mannans and induction of Th17 cell differentiation is essential for host defense against Candida albicans, Immunity 32 (2010) 681–691.
[8] B.N. Gantner, R.M. Simmons, D.M. Underhill, Dectin-1 mediates macrophage recognition of Candida albicans yeast but not filaments, EMBO J. 24 (2005) 1277–1286.
[9] A. Roeder, C.J. Kirschning, R.A. Rupec, M. Schaller, G. Weindl, H.C. Korting, Toll-like receptors as key mediators in innate antifungal immunity, Med. Mycol. 42 (2004) 485–498.
[10] S. Vautier, D.M. MacCallum, G.D. Brown, C-type lectin receptors and cytokines in fungal immunity, Cytokine 58 (2012) 89–99.
[11] K. Sato, X.L. Yang, T. Yudate, J.S. Chung, J. Wu, K. Luby-Phelps, R.P. Kimberly, D. Underhill, P.D. Cruz Jr., K. Ariizumi, Dectin-2 is a pattern recognition receptor for fungi that couples with the Fc receptor gamma chain to induce innate immune responses, J. Biol. Chem. 281 (2006) 38854–38866.
[12] L. Romani, Immunity to fungal infections, Nat. Rev. Immunol. 11 (2011) 275–288.
[13] X. Zhao, Y. Guo, C. Jiang, Q. Chang, S. Zhang, T. Luo, B. Zhang, X. Jia, M.C. Hung, C. Dong, X. Lin, JNK1 negatively controls antifungal innate immunity by suppressing CD23 expression, Nat. Med. 23 (2017) 337–346.
[14] D. Alsina-Beauchamp, A. Escos, P. Fajardo, D. Gonzalez-Romero, E. Diaz-Mora, A. Risco, M.A. Martin-Serrano, C. Del Fresno, J. Dominguez-Andres, N. Aparicio, R. Zur, N. Shpiro, G.D. Brown, C. Ardavin, M.G. Netea, S. Alemany, J.J. Sanz-Ezquerro, A. Cuenda, Myeloid cell deficiency of p38gamma/p38delta protects against candidiasis and regulates antifungal immunity, EMBO Mol. Med. 10 (2018).
[15] M.R. Shakespear, M.A. Halili, K.M. Irvine, D.P. Fairlie, M.J. Sweet, Histone deacetylases as regulators of inflammation and immunity, Trends Immunol. 32 (2011) 335–343.
[16] C. Yanginlar, C. Logie, HDAC11 is a regulator of diverse immune functions, Biochimica et biophysica acta, Gene regulatory mechanisms 1861 (2018) 54–59.
[17] S.K. Byun, T.H. An, M.J. Son, D.S. Lee, H.S. Kang, E.W. Lee, B.S. Han, W.K. Kim, K. H. Bae, K.J. Oh, S.C. Lee, HDAC11 inhibits myoblast differentiation through repression of MyoD-dependent transcription, Mol. Cell. 40 (2017) 667–676.
[18] T.M. Thole, M. Lodrini, J. Fabian, J. Wuenschel, S. Pfeil, T. Hielscher, A. Kopp-Schneider, U. Heinicke, S. Fulda, O. Witt, A. Eggert, M. Fischer, H.E. Deubzer, Neuroblastoma cells depend on HDAC11 for mitotic cell cycle progression and survival, Cell Death Dis. 8 (2017), e2635.
[19] L. Sun, C. Marin de Evsikova, K. Bian, A. Achille, E. Telles, H. Pei, E. Seto, Programming and regulation of metabolic homeostasis by HDAC11, EBioMedicine 33 (2018) 157–168.
[20] P.L. Leslie, Y.L. Chao, Y.H. Tsai, S.K. Ghosh, A. Porrello, A.E.D. Van Swearingen, E. B. Harrison, B.C. Cooley, J.S. Parker, L.A. Carey, C.V. Pecot, Histone deacetylase 11 inhibition promotes breast cancer metastasis from lymph nodes, Nat. Commun. 10 (2019) 4192.
[21] E. Sahakian, J. Chen, J.J. Powers, X. Chen, K. Maharaj, S.L. Deng, A.N. Achille, M. Lienlaf, H.W. Wang, F. Cheng, A.L. Sodre, A. Distler, L. Xing, P. Perez-Villarroel, S. Wei, A. Villagra, E. Seto, E.M. Sotomayor, P. Horna, J. Pinilla-Ibarz, Essential role for histone deacetylase 11 (HDAC11) in neutrophil biology, J. Leukoc. Biol. 102 (2017) 475–486.
[22] J.B. Shao, X.Q. Luo, Y.J. Wu, M.G. Li, J.Y. Hong, L.H. Mo, Z.G. Liu, H.B. Li, D. B. Liu, P.C. Yang, Histone deacetylase 11 inhibits interleukin 10 in B cells of subjects with allergic rhinitis, Int. Forum Allergy Rhinol. 8 (2018) 1274–1283.
[23] A. Villagra, F. Cheng, H.W. Wang, I. Suarez, M. Glozak, M. Maurin, D. Nguyen, K. L. Wright, P.W. Atadja, K. Bhalla, J. Pinilla-Ibarz, E. Seto, E.M. Sotomayor, The histone deacetylase HDAC11 regulates the expression of interleukin 10 and immune tolerance, Nat. Immunol. 10 (2009) 92–100.
[24] D.M. Woods, K.V. Woan, F. Cheng, A.L. Sodre, D. Wang, Y. Wu, Z. Wang, J. Chen, J. Powers, J. Pinilla-Ibarz, Y. Yu, Y. Zhang, X. Wu, X. Zheng, J. Weber, W. W. Hancock, E. Seto, A. Villagra, X.Z. Yu, E.M. Sotomayor, T cells lacking HDAC11

have increased effector functions and mediate enhanced alloreactivity in a murine model, Blood 130 (2017) 146–155.
[25] J. Cao, L. Sun, P. Aramsangtienchai, N.A. Spiegelman, X. Zhang, W. Huang, E. Seto, H. Lin, HDAC11 regulates type I interferon signaling through defatty-acylation of SHMT2, Proc. Natl. Acad. Sci. U.S.A. 116 (2019) 5487–5492.
[26] O. Gross, A. Gewies, K. Finger, M. Schafer, T. Sparwasser, C. Peschel, I. Forster, J. Ruland, Card9 controls a non-TLR signalling pathway for innate anti-fungal immunity, Nature 442 (2006) 651–656.
[27] P.R. Taylor, S.V. Tsoni, J.A. Willment, K.M. Dennehy, M. Rosas, H. Findon, K. Haynes, C. Steele, M. Botto, S. Gordon, G.D. Brown, Dectin-1 is required for beta-glucan recognition and control of fungal infection, Nat. Immunol. 8 (2007) 31–38.
[28] G. Wirnsberger, F. Zwolanek, T. Asaoka, I. Kozieradzki, L. Tortola, R.A. Wimmer, A. Kavirayani, F. Fresser, G. Baier, W.Y. Langdon, F. Ikeda, K. Kuchler, J. M. Penninger, Inhibition of CBLB protects from lethal Candida albicans sepsis, Nat. Med. 22 (2016) 915–923.
[29] R.P. Gazendam, A. van de Geer, D. Roos, T.K. van den Berg, T.W. Kuijpers, How neutrophils kill fungi, Immunol. Rev. 273 (2016) 299–311.
[30] G. Boivin, J. Faget, P.B. Ancey, A. Gkasti, J. Mussard, C. Engblom, C. Pfirschke, C. Contat, J. Pascual, J. Vazquez, N. Bendriss-Vermare, C. Caux, M.C. Vozenin, M. J. Pittet, M. Gunzer, E. Meylan, Durable and controlled depletion of neutrophils in mice, Nat. Commun. 11 (2020) 2762.
[31] G.D. Brown, Innate antifungal immunity: the key role of phagocytes, Annu. Rev. Immunol. 29 (2011) 1–21.
[32] M. Wuthrich, G.S. Deepe Jr., B. Klein, Adaptive immunity to fungi, Annu. Rev. Immunol. 30 (2012) 115–148.
[33] W.K. Alderton, C.E. Cooper, R.G. Knowles, Nitric oxide synthases: structure, function and inhibition, Biochem. J. 357 (2001) 593–615.
[34] M.B. Feldman, J.M. Vyas, M.K. Mansour, It takes a village: phagocytes play a central role in fungal immunity, Semin. Cell Dev. Biol. 89 (2019) 16–23.
[35] Z. Yu, W. Zhang, B.C. Kone, Signal transducers and activators of transcription 3 (STAT3) inhibits transcription of the inducible nitric oxide synthase gene by interacting with nuclear factor kappaB, Biochem. J. 367 (2002) 97–105.
[36] Z. Hou, J. Chen, H. Yang, X. Hu, F. Yang, PIAS1 alleviates diabetic peripheral neuropathy through SUMOlation of PPAR-gamma and miR-124-induced downregulation of EZH2/STAT3, Cell Death Dis. 7 (2021) 372.
[37] L. Li, B. Sun, Y. Gao, H. Niu, H. Yuan, H. Lou, STAT3 contributes to lysosomal-mediated cell death in a novel derivative of riccardin D-treated breast cancer cells in association with TFEB, Biochem. Pharmacol. 150 (2018) 267–279.
[38] D. De Stefano, M.C. Maiuri, B. Iovine, A. Ialenti, M.A. Bevilacqua, R. Carnuccio, The role of NF-kappaB, IRF-1, and STAT-1alpha transcription factors in the iNOS gene induction by gliadin and IFN-gamma in RAW 264.7 macrophages, J. Mol. Med. (Berl.) 84 (2006) 65–74.
[39] H. Kleinert, A. Pautz, K. Linker, P.M. Schwarz, Regulation of the expression of inducible nitric oxide synthase, Eur. J. Pharmacol. 500 (2004) 255–266.
[40] G.R. Stark, J.E. Darnell Jr., The JAK-STAT pathway at twenty, Immunity 36 (2012) 503–514.
[41] M. Gupta, J.J. Han, M. Stenson, L. Wellik, T.E. Witzig, Regulation of STAT3 by histone deacetylase-3 in diffuse large B-cell lymphoma: implications for therapy, Leukemia 26 (2011) 1356–1364.
[42] M.W. Martin, J.Y. Lee, D.R. Lancia Jr., P.Y. Ng, B. Han, J.R. Thomason, M.S. Lynes, C.G. Marshall, C. Conti, A. Collis, M.A. Morales, K. Doshi, A. Rudnitskaya, L. Yao, X. Zheng, Discovery of novel N-hydroxy-2-arylisoindoline-4-carboxamides as potent and selective inhibitors of HDAC11, Bioorg. Med. Chem. Lett 28 (2018) 2143–2147.
[43] S.I. Son, J. Cao, C.L. Zhu, S.P. Miller, H. Lin, Activity-guided design of HDAC11-specific inhibitors, ACS Chem. Biol. 14 (2019) 1393–1397.
[44] J. Chen, F. Cheng, E. Sahakian, J. Powers, Z. Wang, J. Tao, E. Seto, J. Pinilla-Ibarz, E.M. Sotomayor, HDAC11 regulates expression of C/EBPbeta and immunosuppressive molecules in myeloid-derived suppressor cells, J. Leukoc. Biol. 109 (2021) 891–900.
[45] C. Long, Y. Lai, T. Li, T. Nyunoya, C. Zou, Cigarette smoke extract modulates Pseudomonas aeruginosa bacterial load via USP25/HDAC11 axis in lung epithelial cells, Am. J. Physiol. Lung Cell Mol. Physiol. 318 (2020) L252–L263.
[46] M.D. Shahbazian, M. Grunstein, Functions of site-specific histone acetylation and deacetylation, Annu. Rev. Biochem. 76 (2007) 75–100.
[47] C.J. Queval, O.-R. Song, N. Deboosère, V. Delorme, A.-S. Debrie, R. Iantomasi, R. Veyron-Churlet, S. Jouny, K. Redhage, G. Deloison, A. Baulard, M. Chamaillard, C. Locht, P. Brodin, STAT3 represses nitric oxide synthesis in human macrophages upon Mycobacterium tuberculosis infection, Sci. Rep. 6 (2016).
[48] Z.-l. Yuan, Y.-j. Guan, D. Chatterjee, Y.E. Chin, Stat3 dimerization regulated by reversible acetylation of a single lysine residue, Science 307 (2005) 269–273.
[49] S. Ray, C. Lee, T. Hou, I. Boldogh, A.R. Brasier, Requirement of histone deacetylase1 (HDAC1) in signal transducer and activator of transcription 3 (STAT3) nucleocytoplasmic distribution, Nucleic Acids Res. 36 (2008) 4510–4520.